Archival Report

Biological Psychiatry

Noninvasive Modulation of the Subcallosal Cingulate and Depression With Focused Ultrasonic Waves

Thomas S. Riis, Daniel A. Feldman, Sarah S. Kwon, Lily C. Vonesh, Vincent Koppelmans, Jefferson R. Brown, Daniela Solzbacher, Jan Kubanek, and Brian J. Mickey

ABSTRACT

BACKGROUND: Severe forms of depression have been linked to excessive subcallosal cingulate cortex (SCC) activity. Stimulation of the SCC with surgically implanted electrodes can alleviate depression, but current noninvasive techniques cannot directly and selectively modulate deep targets. We developed a new noninvasive neuromodulation approach that can deliver low-intensity focused ultrasonic waves to the SCC.

METHODS: Twenty-two individuals with treatment-resistant depression participated in a randomized, double-blind, sham-controlled study. Ultrasonic stimulation was delivered to the bilateral SCC during concurrent functional magnetic resonance imaging to quantify target engagement. Mood state was measured with the Sadness subscale of the Positive and Negative Affect Schedule before and after 40 minutes of real or sham SCC stimulation. Change in depression severity was measured with the 6-item Hamilton Depression Rating Scale at 24 hours and 7 days.

RESULTS: Functional magnetic resonance imaging demonstrated a target-specific decrease in SCC activity during stimulation ($p = .028$, $n = 16$). In 7 of 16 participants, SCC neuromodulation was detectable at the individual participant level with a single 10-minute scan ($p < .05$, small-volume correction). Mood and depression scores improved more with real than with sham stimulation. In the per-protocol sample ($n = 19$), real stimulation was superior to sham for 6-item Hamilton Depression Rating Scale scores at 24 hours and for Sadness scores (both $p < .05$, $d > 1$). Nonsignificant trends were found in the intent-to-treat sample.

CONCLUSIONS: This small pilot study indicates that ultrasonic stimulation modulates SCC activity and can rapidly reduce depressive symptoms. The capability to noninvasively and selectively target deep brain areas creates new possibilities for the future development of circuit-directed therapeutics and for the analysis of deep-brain circuit function in humans.

https://doi.org/10.1016/j.biopsych.2024.09.029

Deep neural circuits are implicated in the pathophysiology of numerous psychiatric illnesses including mood disorders, anxiety disorders, and addictions. Current treatments for these illnesses are often ineffective, but better therapeutic approaches may be possible through specific and precise modulation of the activity of deep neural targets. For example, severe depression has been linked to excessive activity of the subcallosal cingulate cortex (SCC), a limbic region situated ventral to the corpus callosum (1). Functional imaging studies (1–4) have shown that the SCC is hyperactive in individuals with depression, and interventional studies (5–8) indicate that disruption of SCC activity by deep brain stimulation (DBS) can relieve depressive symptoms.

However, current approaches to DBS require surgical implantation of stimulation leads, which carries considerable risks (9) and high costs that limit the spectrum of individuals who could benefit. In contrast, current noninvasive neuromodulation modalities are limited in other ways. Transcranial magnetic and electric stimulation cannot directly and selectively modulate deep structures such as the SCC due to fundamental physical limitations of electromagnetic fields. This lack of selectivity leads to limited effectiveness and excessive adverse effects.

To address these limitations, we have developed an approach and a device that can modulate the SCC and other deep targets noninvasively and precisely (10–13). The device uses ultrasound transducer arrays to focus low-intensity ultrasonic waves into deep brain targets through the intact skull and scalp (11). Critically, the device measures and compensates for the substantial aberrations of ultrasound by the human head, thus delivering a controlled, deterministic, and safe ultrasound intensity into the target (10).

Here, we applied this new approach to a cohort of participants with treatment-resistant depression using a randomized, blind, sham-controlled study design. Ultrasonic stimulation was delivered to the SCC using individualized magnetic

ISSN: 0006-3223

resonance imaging (MRI) guidance, and the neural effects of stimulation were quantified using concurrent functional MRI. The 2 parallel objectives of the study were 1) to demonstrate that ultrasonic stimulation engages the SCC target and 2) to characterize the immediate mood effects and tolerability of this stimulation. We hypothesized that SCC sonication would deactivate the SCC and improve mood and depressive symptoms.

METHODS AND MATERIALS

Study Design and Participants

This study was approved by the University of Utah Institutional Review Board, monitored by an independent safety monitor, and preregistered on clinicaltrials.gov (NCT05301036). All participants provided written informed consent. Eligible individuals were adults (ages 18–65 years) with a primary DSM-5 diagnosis of major depressive disorder or bipolar disorder and a current moderate-to-severe depressive episode without psychotic features lasting at least 2 months (see Table S1 for full inclusion/exclusion criteria). This pilot study incorporated a double-blind, randomized, sham-controlled, crossover design (Figure 1). Clinical evaluation was performed at the baseline visit, and approximately 1 week later, the participant returned for the first stimulation visit, where they were randomized 1:1 to the real-stimulation or sham-stimulation arm. At the first stimulation visit, each subject participated in a 1-hour MRI session followed immediately by a 1-hour treatment session. Seven days later, each participant returned for the second stimulation visit, where participants crossed over from real to sham or from sham to real. At the second stimulation visit, the 1-hour MRI session and 1-hour treatment session were repeated. Symptoms were assessed at the start and end of each stimulation visit and 24 hours and 7 days following each stimulation visit. The prespecified enrollment target was 20 participants with analyzable data. As shown in Figure S1, 29 participants were enrolled, 22 were randomized, and 20 crossed over. The 2 participants described previously (10–12) are not included in this report.

Ultrasound Device

The ultrasound device and approach are fully described in Supplemental Methods and recent publications (10,11). Briefly, 2 ultrasound transducer phased arrays were situated in a frame over the left and right sides of the head. Acoustic coupling gels were placed between each array and the head, and a thermoplastic mask was individually fit to the participant's head to minimize movement relative to the frame and transducer arrays. A transmit-receive scan was performed between the 2 arrays to measure the acoustic distortion caused by the head and coupling, and an algorithm calculated phase and amplitude adjustments at each transducer element that fully compensated for the distortion. MRI was performed with the ultrasound transducer arrays locked in place, and the arrays were coregistered to the individual's brain anatomy using fiducial markers on the device that were visible in the MRI. The device created a sonication focus that extended 20.4 × 2.4 × 3.6 mm (x, y, z dimensions in Montreal Neurological Institute space). The focus was moved to the desired target programmatically without moving the device or participant. To assure safety, ultrasound intensities were always delivered below the Food and Drug Administration 510(k) Track 3 guidelines for diagnostic ultrasound (peak intensity $<$190 W/cm^2, time-averaged intensity $<$720 mW/cm^2, mechanical index $<$1.9) (14).

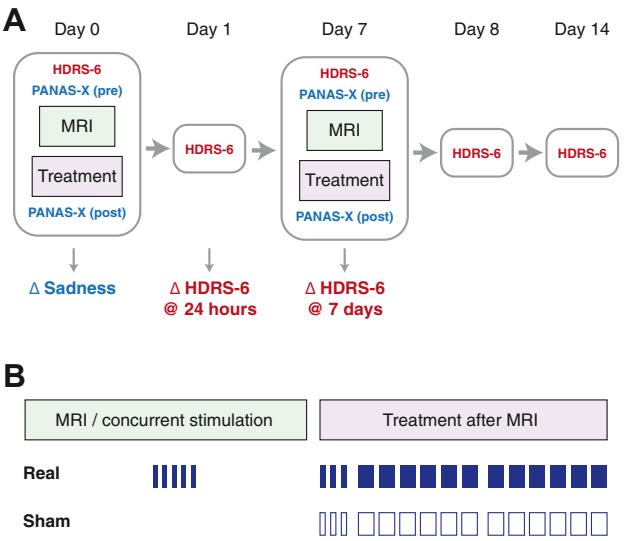

Figure 1. Study design. This pilot study incorporated a double-blind, randomized, sham-controlled, crossover design. **(A)** Overall design. Approximately 1 week after a baseline visit (not shown), the participant returned for the first stimulation visit (day 0), where they were randomized 1:1 to the real-stimulation or sham-stimulation arm. Pretreatment scales were collected: the 6-item Hamilton Depression Rating Scale (HDRS-6) and expanded Positive and Negative Affect Schedule (PANAS-X). Each participant then participated in a 1-hour magnetic resonance imaging (MRI) session followed immediately by a 1-hour treatment session. A posttreatment PANAS-X was completed immediately after the treatment session. The HDRS-6 was repeated 24 hours later (day 1). Participants returned 6 days later (day 7) when their treatment assignment crossed over to sham or real, and the procedures of day 0 were repeated. The HDRS-6 was repeated 24 hours and 7 days later (day 8 and day 14). The primary efficacy outcomes, shown at the bottom of the panel, were change in PANAS-X sadness score on day 0, change in HDRS-6 score from day 0 to day 1, and change in HDRS-6 score from day 0 to day 7. **(B)** Detail for days 0 and 7. Participants who were randomized to real stimulation on day 0 received five 1-minute trials of active ultrasonic stimulation (filled rectangles) during concurrent blood oxygen level–dependent imaging to measure target engagement. The MRI session was followed immediately by the treatment session, during which the participant received a series of 1- and 3-minute active ultrasonic stimulation trials (filled rectangles). Participants who were randomized to the sham intervention had MRI without stimulation, followed immediately by a series of 1- and 3-minute sham stimulation trials (open rectangles). Continuous white noise was delivered during the MRI for both real and sham interventions. Custom-designed auditory masking stimuli timed to coincide with ultrasound delivery were played via earbuds during the treatment session for both real and sham arms. Similar protocols were repeated on day 7 after crossover.

Targeting and Measurement of Target Engagement

The individual's T1-weighted image was used to guide ultrasound targeting. Blood oxygen level–dependent (BOLD) imaging was used to measure target engagement. Details of MRI acquisition are provided in Supplemental Methods. The center

of the sonication focus was positioned on the midline, spanning the left and right SCC, to approximate bilateral targets that have been described previously for invasive DBS (15). Individual targets are shown in Figure S2. Ultrasound was delivered with an amplitude of 1 MPa at target [31.1 W/cm^2; following skull correction (10)], 30-ms burst duration containing pulses of 5 ms on and 5 ms off, separated by 1.4-second burst intervals, for 60 seconds. These stimulus parameters were expected to cause net inhibitory effects (16,17). Neuromodulation was quantified using concurrent (online) BOLD imaging with a 10-minute block-design paradigm consisting of five 1-minute rest epochs (no sonication) interleaved with five 1-minute epochs of active sonication. Continuous white noise was played throughout the 10-minute session via earbuds with the goal of masking any potential auditory effects caused by the ultrasound. Because of technical difficulties during some BOLD imaging sessions, in several cases, it was necessary to deviate from protocol and repeat real stimulation during functional MRI at the second stimulation session even though treatment assignment had crossed over from real to sham (see Supplemental Methods). Usable BOLD data were not obtainable from 5 of 21 participants who received sonication during MRI due to technical problems, so the final dataset reported here includes a total of 16 participants.

Randomization and Blinding

Participants were randomized to real (active) or sham (placebo) groups when they arrived for the first stimulation visit. The device operator was necessarily unblinded to allocation at the first stimulation visit. All other staff, participants, and clinical raters remained blinded. Treatment allocation was disclosed to participants following the 6-item Hamilton Depression Rating Scale (HDRS-6) rating, which occurred 7 days after the second stimulation visit. The effectiveness of blinding was assessed by asking a subset of 13 participants to guess which intervention they received. See Supplemental Methods for details.

Real and Sham Treatment Sessions

Immediately after MRI with concurrent stimulation, additional stimulation was delivered outside the scanner during a single 1-hour treatment session that included 39 to 41 minutes (cumulative) of real or sham sonication (Figure 1). Because the optimal target was not known with millimeter precision, 3 adjacent midline targets within the SCC region were stimulated sequentially with the goal of maximizing changes in mood symptoms. In addition to the original target stimulated during concurrent functional MRI, 2 targets approximately 4-mm anterior and 4-mm posterior were defined on the individual MRI. These 3 SCC targets (anterior, middle, posterior) were then stimulated for equal duration, in random order, over a 1-hour session. Ultrasound was delivered to each target with an amplitude of 1 MPa [31.1 W/cm^2; following skull correction (10)], with a 30-ms burst duration containing pulses of 5 ms on and 5 ms off separated by 1.4- or 0.7-second burst intervals. Overall, the treatment session consisted of 3 blocks (A, B, C), each of which included stimulation of all 3 targets. Block A contained three to five 1-minute sonications to test the tolerability of each target with 1.4-second burst intervals. Block B contained six 3-minute sonications with 1.4-second burst intervals. Block C contained six 3-minute sonications with 0.7-second burst intervals.

To mask the faint vibratory percepts sometimes experienced with ultrasound stimulus delivery (18,19), participants wore earbuds and received identical auditory stimuli during both active and sham interventions. White noise was combined with audio recordings of ultrasound pulses from the arrays, and auditory stimuli were timed to coincide with delivery of ultrasound stimulation.

Clinical Outcome Measures

Two coprimary efficacy measures were prespecified. The Sadness subscale of the expanded Positive and Negative Affect Schedule (PANAS-X) quantified immediate change in mood state, and the HDRS-6 measured changes in depressive symptom severity at 24 hours and 7 days (see Figure 1). The PANAS-X is a reliable, validated, 60-item self-report measure of mood state (20). The HDRS-6 is an abbreviated version of the original 17-item instrument (21) that correlates with longer versions of the HDRS, is sensitive to change, and unlike the 17-item scale can be applied to brief time frames, thus allowing measurement of rapid effects (22–25). Tolerability and safety were assessed at each visit through collection of spontaneously reported adverse events, the General Assessment of Side Effects scale (26), the Young Mania Rating Scale, and the Columbia-Suicide Severity Rating Scale. Secondary outcomes included the self-reported Inventory of Depressive Symptomatology and 7-item Generalized Anxiety Disorder scale. Details are described in the Supplement.

Functional MRI Analysis

The functional MRI processing pipeline is described in Supplemental Methods. Whole-brain data from a single 10-minute scan was analyzed for each participant using a standard first-level SPM12 general linear model. The first-level model employed a block design that contrasted five 1-minute ON epochs (active ultrasonic stimulation) with five 1-minute OFF epochs (no stimulation). Fitting of this model produced whole-brain beta weight maps for ON>OFF and OFF>ON, as well as corresponding t statistic maps, at each voxel.

The primary analysis of target engagement used a region of interest (ROI) corresponding to the SCC volume where ultrasound was delivered (described in Supplemental Methods). To evaluate target engagement for each participant, SPM12 familywise error small-volume correction was applied to the participant's t statistic maps (ON>OFF and OFF>ON) using the SCC ROI. This produced 1-tailed p values for activation (ON>OFF) and deactivation (OFF>ON) of the SCC for that participant. A threshold of $p < .025$ for either activation or deactivation was considered significant (equivalent to a single 2-tailed t test with a conventional threshold of $p < .05$). To evaluate target engagement at a group level, a second-level ON>OFF group model was constructed, and collapsed beta weights were extracted from the SCC ROI for each participant. A 2-tailed 1-sample t test was applied to these extracted beta weights, and $p < .05$ was considered significant. Analysis of brainwide effects is described in Supplemental Methods.

Analysis of Clinical Outcomes

Change in PANAS-X Sadness (post- minus prestimulation) at the first stimulation visit was calculated for each participant, and the difference between treatment groups (real vs. sham) was evaluated using a 2-sample *t* test. Similarly, changes in HDRS-6 scores 24 hours and 7 days after the first stimulation visit were calculated, and 2-sample *t* tests were applied to test for group differences at each time point.

The intention-to-treat sample included all 22 participants who were randomized. The per-protocol sample (n = 19) excluded 3 participants who received stimulation other than as intended in the prespecified protocol. One participant had received active stimulation during MRI under a different protocol prior to being randomized to the real arm; 1 participant received active stimulation during MRI despite being randomized to the sham arm; and 1 participant inadvertently received several minutes of active stimulation during the sham treatment session.

RESULTS

Characteristics of Participants

Twenty-nine adults with treatment-resistant depression enrolled in the study, and 22 were randomized (see CONSORT [Consolidated Standards of Reporting Trials] diagram, Figure S1). Ten were assigned to receive real stimulation at the first session, and 12 were assigned to receive sham stimulation. Demographic and clinical characteristics were comparable for the real- and sham-stimulation groups (all $ps > .05$) (Table 1). Twenty participants returned for a second stimulation visit to cross over to the other condition (sham or real).

Target Engagement

Individual-level analyses showed statistically significant neuromodulation in the targeted SCC region in 7 of 16 participants ($p < .05$, familywise error small-volume correction) based on a single 10-minute BOLD imaging session (Table S2). For 5 participants, the expected decrease in BOLD signal (i.e., deactivation) was detected. An example of the SCC deactivation is shown in Figure 2A–C. Nine participants showed no significant modulation, and 2 participants showed significant activation of the SCC. At the group level, the average effect of the SCC modulation was deactivation: beta weights extracted from the SCC ROI (Figure 2D) were significantly less than zero across the cohort ($t_{15} = -2.43$, $p = .028$, 1-sample 2-tailed *t* test).

Brainwide Effects

To evaluate the broader effects of SCC modulation on brain networks, we evaluated the effects across the brain in each participant. Diverse patterns of activation and deactivation were observed in distributed brain regions (Figure S3). At the group level, whole-brain analysis revealed no consistent deactivation beyond the SCC ($p > .05$, false discovery rate corrected). However, activation (i.e., an increase in activity) was detected at a group level in the left ventrolateral prefrontal cortex and right superior temporal gyrus (Table S3).

Responses in distributed brain areas may depend on the polarity of the SCC modulation. Therefore, we also analyzed the subset of 12 participants for whom sonication deactivated the SCC. Significant deactivation was found only in the SCC (Figure 3). Activation was detected in the left ventrolateral

Table 1. Baseline Demographic and Clinical Features of the Intent-to-Treat Sample

	Real Stimulation, n = 10	Sham Stimulation, n = 12	All Participants, N = 22
Demographics			
Age, Years	37.37 (11.85)	41.23 (8.41)	39.47 (10.05)
Gender, Female	6 (60%)	8 (67%)	14 (64%)
Non-Hispanic White	7 (70%)	10 (83%)	17 (77%)
Education, Years	15.9 (1.10)	15.83 (1.64)	15.86 (1.39)
Diagnoses and Comorbidities			
Primary DSM-5 Diagnosis			
Major depressive disorder	9 (90%)	11 (92%)	20 (91%)
Bipolar disorder	1 (10%)	1 (8%)	2 (9%)
Generalized Anxiety Disorder	4 (40%)	7 (58%)	11 (50%)
Panic Disorder	2 (20%)	4 (33%)	6 (27%)
Agoraphobia	3 (30%)	1 (8%)	4 (18%)
Social Anxiety Disorder	4 (40%)	5 (42%)	9 (41%)
Obsessive-Compulsive Disorder	2 (20%)	1 (8%)	3 (14%)
Posttraumatic Stress Disorder	4 (40%)	2 (17%)	6 (27%)
Alcohol Use Disorder, Mild	0 (0%)	1 (8%)	1 (5%)
Other Substance Use Disorder, Mild	2 (20%)	0 (0%)	2 (9%)
Lifetime History of Psychosis	0 (0%)	1 (8%)	1 (5%)
Severity Scales			
HDRS-6	12.00 (2.91)	11.42 (1.38)	11.68 (2.17)
IDS-SR	43.90 (9.80)	44.42 (9.62)	44.18 (9.47)
QIDS-SR	17.10 (3.28)	18.33 (3.11)	17.77 (3.18)
YMRS	1.10 (1.20)	1.00 (0.85)	1.05 (1.00)
GAD-7	12.60 (5.80)	10.00 (5.38)	11.18 (5.59)
Chronicity and Resistance			
Age of Onset, Years	17.70 (5.25)	14.33 (5.82)	15.86 (5.70)
Duration of Current Episode, Months, Median (IQR)	13.00 (12.00)	24.00 (27.50)	20.00 (23.25)
Chronic Episode, >24 Months	4 (40%)	6 (50%)	10 (45%)
Failed Antidepressant Trials, Current Episode	1.60 (0.70)	1.42 (1.24)	1.50 (1.01)
Maudsley Staging Method	7.40 (1.58)	7.42 (1.38)	7.41 (1.44)

Values are presented as mean (SD) or n (%) unless indicated otherwise. Diagnoses were determined with the Mini-International Neuropsychiatric Interview, version 7.0. Two participants with bipolar disorder had a history of subthreshold manic symptoms that did not meet criteria for bipolar I or II disorder. Only clearly documented failed antidepressant medication trials in the past 2 years were included. No significant differences were found between real and sham groups (all $ps > .05$).

HDRS-6, 6-item Hamilton Depression Rating Scale; GAD-7, 7-item Generalized Anxiety Disorder; IDS-SR, Inventory of Depressive Symptomatology, Self-Report; QIDS-SR, Quick Inventory of Depressive Symptomatology, Self-Report; YMRS, Young Mania Rating Scale.

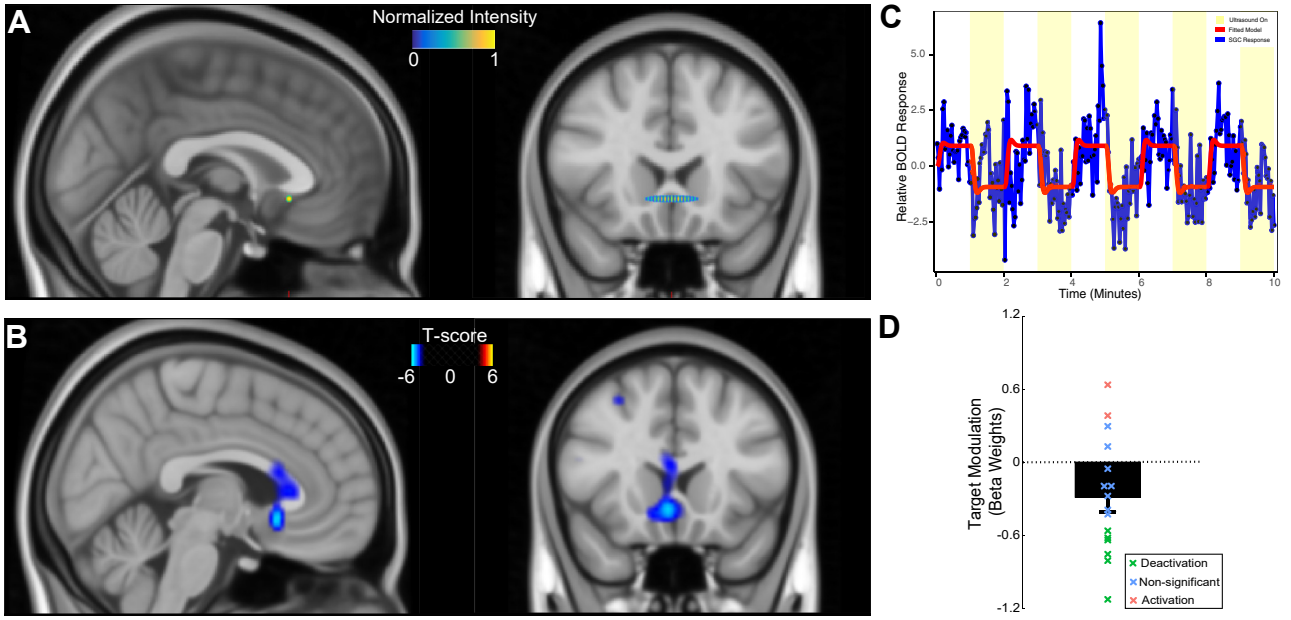

Figure 2. Ultrasonic targeting and neuromodulation. **(A)** Calculated ultrasound field produced at focus overlaid on sagittal and coronal images. The dimensions of the focus are 20.4 × 2.4 × 3.6 mm (Montreal Neurological Institute space). **(B)** Target engagement in an individual participant, assessed using concurrent blood oxygen level–dependent (BOLD) imaging. The subcallosal cingulate cortex (SCC) was selectively deactivated: peak coordinates = (4, 20, −6), SCC small volume–corrected $p < .001$ and whole-brain familywise error–corrected $p < .001$. Display thresholds: $|t| > 4$, cluster size > 50 voxels. **(C)** SCC BOLD response from the example participant in **(B)** (blue) and fitted block-design model (red) are shown. BOLD signal decreased with ultrasound delivery (yellow). **(D)** Modulation of the targeted SCC region across the cohort ($n = 16$). Each symbol represents the BOLD response extracted from the SCC for an individual participant. The bar shows the mean ± SEM response: $t_{15} = -2.43$, $p = .028$, 1-sample 2-tailed t test. The symbol colors indicate individual participant results from small-volume correction analyses (see Table S2). Statistically significant deactivation was observed at the individual participant level in 5 participants, and 1 participant trended toward deactivation (green). Two participants showed a significant activation (red). In 8 participants (blue), the modulation was not significant at the individual level. SGC, subgenual cingulate cortex.

prefrontal cortex and bilateral temporal cortex (Table S3), consistent with the findings for the full cohort.

Changes in Mood and Depression

The primary efficacy end points were change in PANAS-X Sadness score immediately following stimulation and change in HDRS-6 score 24 hours and 7 days following the stimulation visit.

In the per-protocol sample ($n = 19$), the group difference for change in the Sadness score was statistically significant ($p = .027$, $t_{16} = -2.43$, $d = -1.15$), as shown in Figure 4. Pretreatment Sadness scores were higher for the real-stimulation group than for the sham-stimulation group (56.1 vs. 39.5), but the difference was not statistically significant; posttreatment Sadness scores also did not differ by treatment group (Table S5).

In the per-protocol sample, change in HDRS-6 scores was significant at 24 hours ($p = .031$, $t_{17} = -2.35$, $d = -1.08$) but not at 7 days ($p = .22$, $t_{17} = -1.29$, $d = -0.59$), as shown in Figure 5. The rate of response (improvement ≥ 50% in HDRS-6 scores) for sham versus active stimulation was 20% versus 67% at 24 hours and 30% versus 67% at 7 days (Figure 5E).

For the intent-to-treat sample ($n = 22$), scores decreased more in the real-stimulation group than the sham-stimulation group, but group differences did not reach significance for

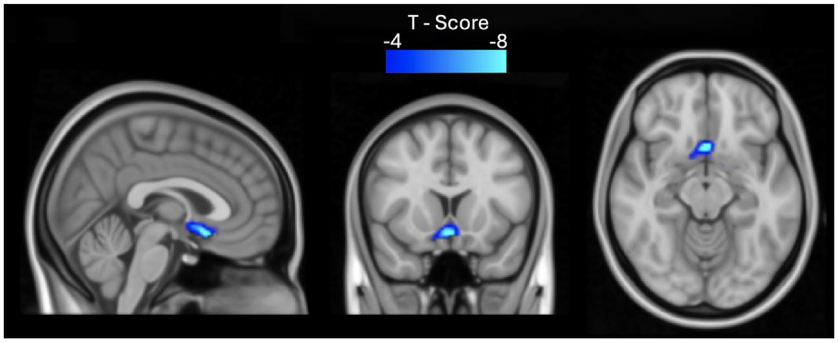

Figure 3. Selective deactivation of the subcallosal cingulate cortex. Group analysis performed on the 12 participants who showed a deactivation of the subcallosal cingulate cortex during stimulation. The corresponding negative beta weights are shown in Figure 2D. No other regions were significantly deactivated.

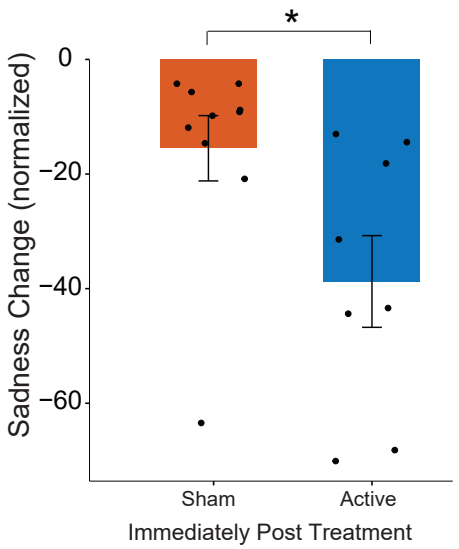

Figure 4. Improvements in mood following ultrasonic modulation of the subcallosal cingulate cortex. Immediate change in expanded Positive and Negative Affect Schedule (PANAS-X) sadness score with treatment for sham stimulation (n = 10) vs. active stimulation (n = 8) for the per-protocol sample. The mean percentage change in the sadness score was −63% in the active group vs. −47% in the sham group. Between-groups standardized effect size d = −1.15 (95% CI, −2.24 to −0.07). *p < .05. Data points indicate individual participants. Error bars denote SEM.

the sadness score (p = .064, t_{19} = −1.96, d = −0.87), HDRS-6 at 24 hours (p = .18, t_{20} = −1.38, d = −0.59), or HDRS-6 at 7 days (p = .45, t_{20} = −0.77, d = −0.33).

Tolerability and Safety

During this crossover study, 21 participants received real stimulation, and 21 participants received sham stimulation. No serious adverse events occurred during the course of the study. No severe adverse events occurred during or immediately after stimulation. No participants experienced mania or hypomania.

At follow-up visits 24 hours after each stimulation visit, self-reported side effects were measured with a standardized questionnaire (Table 2). The symptoms that were most commonly reported were depressed mood (real, 62%; sham, 67%), headache (real, 57%; sham, 67%), and anxiety (real, 57%; sham, 52%). Suicidal thoughts were reported by 29% of participants after real stimulation and 24% of participants after sham stimulation.

Two participants experienced a severe psychiatric adverse event with onset later than the 24-hour follow-up visit, both of which followed real stimulation. The first participant developed acute depression with suicidal ideation 3 days after stimulation and took an intentional overdose of medication that did not require medical intervention. The other participant developed rapid worsening of depression with suicidal ideation a few hours after the 24-hour follow-up visit. Both participants had a history of similar mood swings. Over the subsequent 2 weeks, depression improved and suicidal ideation resolved for both participants.

Effectiveness of Blinding

At the end of the first stimulation visit, 13 participants were asked to guess which intervention they received on a 0 to 100 scale, with 50 representing complete uncertainty. The mean (SD) rating was 48 (32) for the sham group and 64 (26) for the active group. Neither was significantly different from 50 (p = .87 and p = .30, 1-sample 2-tailed t tests), and mean values for the 2 groups did not differ from each other (p = .35, 2-sample 2-tailed t test). This suggests that the blinding procedures used in this study were effective.

DISCUSSION

Here, we report the first application of a novel neuromodulation approach to a cohort of individuals with treatment-resistant depression. In this approach, a phased array device delivers ultrasound into specified deep brain targets while measuring and compensating for the severe aberrations of ultrasound by the head (10,11). We found that transcranial delivery of low-intensity focused ultrasound to the SCC can safely reduce SCC activity, elicit immediate mood improvement, and rapidly decrease depressive symptoms. This proof-of-principle demonstration suggests that this approach could be developed into an effective, noninvasive, rapidly acting intervention for depression. More generally, the capability to noninvasively, flexibly, and selectively target deep brain areas creates new possibilities for circuit-directed therapeutic interventions for a range of neuropsychiatric disorders.

Precise and noninvasive modulation of deep brain targets in humans has been an elusive goal. Ultrasonic energy has become a prime candidate for attaining this objective (27–29). Ultrasonic waves combine a unique triad of properties—noninvasiveness, depth penetration, and sharp focus. Compared to electromagnetic waves, sound waves have a small wavelength. Thanks to diffraction (30), the short wavelength enables relatively sharp focus at depth. Nonetheless, ultrasonic technology has been impeded by formidable barriers—the skull and hair, which attenuate and distort ultrasonic waves severely and unpredictably (10,31). The approach used here directly measures and compensates for these barriers in each individual, thus delivering into specified targets a controlled, deterministic ultrasound intensity that results in safe and effective neuromodulation (10,11,13).

We hypothesized that sonication of the SCC would reduce activity in the targeted area. This result was confirmed for the group as a whole and for 5 participants with statistically significant deactivation at the individual level (Figure 2D). However, we also observed substantial interindividual variability, with 2 participants showing significant activation of the SCC during sonication. Potential sources of this variability include imperfect correction of ultrasound aberration by the device, millimeter-scale variation in targeting, and individual anatomical or physiological differences. The latter possibility has been highlighted by invasive DBS experiments that indicate that individual tractography may be necessary for optimal placement of electrodes (32). Similar individualized optimization of targeting may be needed with noninvasive focused ultrasound to achieve consistent effects across participants. A major advantage of our method over surgical approaches is that the ultrasound focus is readily steered to a different target without moving the device or participant. Furthermore, multiple targets can be defined and sonicated sequentially or near-simultaneously. The flexibility of this approach, together with

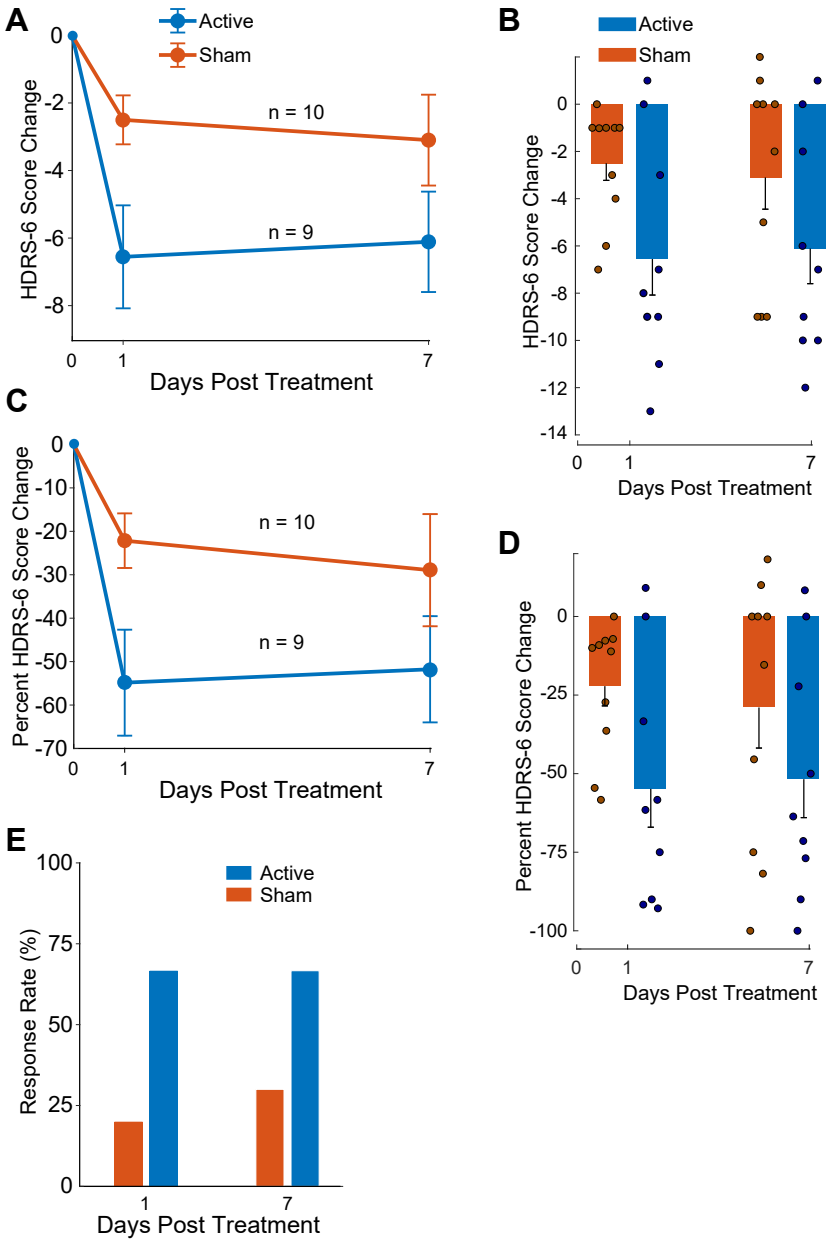

Figure 5. Improvements in depressive symptoms following ultrasonic stimulation of the subcallosal cingulate cortex. **(A)** Change in 6-item Hamilton Depression Rating Scale (HDRS-6) score 24 hours and 7 days posttreatment for the per-protocol sample. Between-groups standardized effect size $d = -1.08$ (95% CI, 2.11 to −0.04) at 24 hours and $d = -0.59$ (95% CI, −1.59 to 0.40) at 7 days. Mean ± SEM is shown. **(B)** Data from **(A)** are plotted again to show data points for individual participants. **(C)** Data from **(A)** are replotted as percentage change relative to pretreatment on day 0. HDRS-6 scores at 1 and 7 days changed by −55% and −52% in the active group and −22% and −29% in the sham group, respectively. Mean ± SEM is shown. **(D)** Data from **(C)** are plotted again to show data points for individual participants. **(E)** The proportion of participants who experienced ≥50% reduction in HDRS-6 score (response rate) is shown at 24 hours and 7 days for the active group ($n = 9$) and sham group ($n = 10$).

the safety of repeated stimulation, lends itself well to individualized optimization. This flexible approach could also be applied to other targets investigated with surgical DBS such as the medial forebrain bundle and ventral striatum (6,7). Furthermore, this noninvasive approach could have potential as a predictive presurgical probe for more refractory patients who are candidates for invasive DBS.

Our findings support the idea that deactivation of the SCC with transcranial ultrasound can cause an immediate decrease in sad mood and a rapid improvement of depressive symptoms in individuals with moderate-to-severe treatment-resistant depression. The differences between active and sham treatment groups were greatest for participants treated per protocol and for the immediate and 24-hour assessments, but durable antidepressant effects lasting 1 week or longer were observed for a subset of participants. Our approach can be compared with previous studies that used single-element transducers to deliver transcranial ultrasound to the frontal lobe with the goal of modulating mood states in individuals with chronic pain (33), in healthy participants (34), and in participants with mild-to-moderate depression (35). Those studies showed limited effectiveness and effect duration. Our approach differs from these previous studies in 3 fundamental ways: 1) we measured and corrected for the ultrasound

Table 2. Stimulation Safety

	Real, n = 21					Sham, n = 21				
GASE Rating	Not Present	Mild	Moderate	Severe	Related to Treatment	Not Present	Mild	Moderate	Severe	Related to Treatment
Headache	9	9	3	0	6 (28.57%)	7	8	5	1	3 (14.29%)
Hair Loss	21	0	0	0	0 (0%)	21	0	0	0	0 (0%)
Dry Mouth	13	7	1	0	1 (4.76%)	13	7	1	0	0 (0%)
Dizziness	17	3	1	0	1 (4.76%)	11	10	0	0	2 (9.52%)
Chest Pain	20	1	0	0	0 (0%)	20	1	0	0	0 (0%)
Palpitations	19	1	1	0	2 (9.52%)	19	2	0	0	1 (4.76%)
Breathing Problems	21	0	0	0	0 (0%)	20	1	0	0	0 (0%)
Subjective Blood Circulation–Associated Problems	19	1	1	0	0 (0%)	20	1	0	0	1 (4.76%)
Abdominal Pain	21	0	0	0	0 (0%)	16	3	2	0	0 (0%)
Nausea	19	2	0	0	0 (0%)	18	2	1	0	0 (0%)
Vomiting	21	0	0	0	0 (0%)	21	0	0	0	0 (0%)
Constipation	18	2	1	0	0 (0%)	13	5	2	1	0 (0%)
Diarrhea	20	1	0	0	0 (0%)	17	4	0	0	0 (0%)
Reduced Appetite	18	2	1	0	1 (4.76%)	16	5	0	0	0 (0%)
Increased Appetite	18	1	2	0	0 (0%)	18	3	0	0	0 (0%)
Difficulty Urinating	21	0	0	0	0 (0)	21	0	0	0	0 (0%)
Problems With Sexual Performance or Sex Organs	21	0	0	0	0 (0%)	21	0	0	0	0 (0%)
Painful or Irregular Menstruation	21	0	0	0	0 (0%)	21	0	0	0	0 (0%)
Skin Rash or Itching	20	1	0	0	0 (0%)	20	1	0	0	0 (0%)
Tendency to Develop Bruises	18	1	2	0	0 (0%)	20	0	1	0	0 (0%)
Fever, Increased Temperature	21	0	0	0	0 (0%)	21	0	0	0	0 (0%)
Abnormal Sweating	20	0	0	1	1 (4.76%)	20	1	0	0	0 (0%)
Hot Flashes	20	0	1	0	1 (4.76%)	18	3	0	0	0 (0%)
Convulsions or Seizures	21	0	0	0	0 (0%)	21	0	0	0	0 (0%)
Fatigue, Loss of Energy	13	3	2	3	3 (14.28%)	12	3	6	0	2 (9.52%)
Tremor	19	1	1	0	0 (0%)	19	2	0	0	0 (0%)
Insomnia, Sleeping Problems	11	7	1	2	1 (4.76%)	15	5	1	0	0 (0%)
Nightmares or Abnormal Dreams	15	2	3	1	1 (4.76%)	18	3	0	0	0 (0%)
Back Pain	14	5	1	1	1 (4.76%)	14	4	3	0	1 (4.76%)
Muscle Pain	16	5	0	0	1 (4.76%)	13	6	1	1	2 (9.52%)
Joint Pain	16	3	1	1	1 (4.76%)	14	6	0	1	2 (9.52%)
Agitation	16	3	2	0	1 (4.76%)	15	4	1	1	1 (4.76%)
Irritability, Nervousness	12	6	2	1	2 (9.52%)	11	7	2	1	1 (4.76%)
Depressed Mood	8	4	6	3	1 (4.76%)	7	6	6	2	1 (4.76%)
Thoughts About Suicide	15	4	1	1	1 (4.76%)	16	3	0	2	1 (4.76%)
Anxiety, Fearfulness	9	8	3	1	1 (4.76%)	10	5	5	1	1 (4.76%)

Values are presented as n or n (%). Twenty-four hours after ultrasonic stimulation, participants completed a standard clinical questionnaire (26) that assessed a range of potential side effects. The data are shown separately for the active (left column) and sham (right column) stimulation.

GASE, General Assessment of Side Effects.

aberrations by the head (10); 2) we focused the ultrasound into the target using phased arrays, which provide focal, precise, and flexible ultrasound delivery (11–13); and 3) we used MRI for guidance and BOLD imaging to validate target engagement. These approaches enabled us to deliver ultrasound into the SCC precisely, selectively, and in a controlled manner. Additional factors, such as the stimulation parameters, targeted structures, and patient profiles, may also contribute to these marked differences.

We found good overall tolerability of SCC sonication and no serious adverse events. No severe problems were observed during or within 24 hours of stimulation, but 2 participants experienced significant mood swings in the period 24 to 72 hours following real SCC stimulation, including clinically significant worsening of suicidal ideation, which resolved over the subsequent 2 weeks. These observations raise the possibility that SCC sonication could elicit delayed adverse psychiatric effects in some individuals. The assessment of causality is complicated by the late onset of these events following stimulation and the lack of adverse clinical response during the first 24 hours. Both participants described a history of similar seemingly unprovoked mood swings in the past. Therefore, the clinical worsening seen following stimulation might have been

coincidental, but it is perhaps more likely that the ultrasonic stimulation or other study procedures triggered neural changes that required 24 to 72 hours to fully manifest. Future studies should monitor the psychiatric status of participants frequently during the week following SCC stimulation.

The current study has several caveats and limitations. First, this pilot study of 22 participants was powered to detect only large effects. Medium-sized but still important effects on target engagement or clinical outcomes were likely missed, and small studies such as this pose a risk of inflated effect-size estimation. Furthermore, small samples are vulnerable to random-chance imbalances in baseline characteristics between groups (such as those we observed with pretreatment sadness scores) that can be a source of confounding. Second, as in previous studies in humans, we used auditory masking. Our functional MRI findings indicate that the auditory cortex is activated bilaterally with active stimulation, consistent with anecdotal reports from participants of auditory percepts associated with sonication. Our evaluation of the effectiveness of blinding suggested that participants were unable to determine which intervention they received, but future studies should verify and optimize the auditory masking protocol and directly compare real versus sham interventions also using functional MRI. Third, the crossover study design limited the formal evaluation of participants to only 7 days following a stimulation session. In a recent case report, we described a participant with treatment-resistant depression who unexpectedly experienced remission that lasted more than 6 weeks (12). Given this finding, systematic studies are needed to evaluate the effect duration over a period of many weeks to optimize the development of practical and effective clinical interventions. Fourth, targeting for this study used only T1-weighted MRI. Previous work on optimization of SCC DBS has shown that targeting differences of a few millimeters can produce diverse therapeutic effects and furthermore that DBS electrodes are more effective when they engage SCC structural connections (32). In future work, we plan to use tractography to optimize SCC targeting. Finally, in this study, we used functional MRI to evaluate target engagement; future studies would benefit from confirmation of ultrasound targeting using mechanical or elastographic methods (36,37).

Conclusions

We provide proof-of-concept evidence that ultrasound can noninvasively modulate deep brain circuits and rapidly improve depressive symptoms. Moreover, this flexible approach offers a new diagnostic and scientific tool to analyze human neural circuitry.

ACKNOWLEDGMENTS AND DISCLOSURES

This work was supported by the National Institute of Health (Grant Nos. R00NS100986, RF1NS128569, S10OD026788, UL1TR002538, and R61MH134943), the University of Utah College of Engineering seed grant, the University of Utah Ascender grant, and the University of Utah Department of Psychiatry.

We thank the Imaging and Neurosciences Center for expert help with MRI acquisition; Courtney Rada for assistance collecting clinical information; and our participants for volunteering for this study.

JK is an inventor on a patent related to the ultrasound device and reports a significant financial interest in SPIRE Therapeutic, which licenses the intellectual property. TSR has a financial interest in and is a consultant for SPIRE Therapeutic. JRB reports a family member with a significant financial interest in SPIRE Therapeutic. BJM has received support from LivaNova, Health Rhythms, Compass Pathways, and Abbott for research unrelated to this work. All other authors report no biomedical financial interests or potential conflicts of interest.

ClinicalTrials.gov: Personalized Ultrasonic Brain Stimulation for Depression: A Pilot Study of Target Engagement and Mood Effects; https://clinicaltrials.gov/study/NCT05301036; NCT05301036.

ARTICLE INFORMATION

From the Department of Biomedical Engineering, University of Utah, Salt Lake City, Utah (TSR, DAF, JK, BJM); Department of Radiology, University of Utah, Salt Lake City, Utah (DAF); and Department of Psychiatry, Huntsman Mental Health Institute, University of Utah, Salt Lake City, Utah (DAF, SSK, LCV, VK, JRB, DS, JK, BJM).

TSR, DAF, JK, and BJM contributed equally to this work.

Address correspondence to Brian J. Mickey, M.D., Ph.D., at brian.mickey@utah.edu, or Thomas S. Riis, Ph.D., at tom.riis@utah.edu.

Received May 5, 2024; revised Sep 19, 2024; accepted Sep 30, 2024.

Supplementary material cited in this article is available online at https://doi.org/10.1016/j.biopsych.2024.09.029.

REFERENCES

1. Hamani C, Mayberg H, Stone S, Laxton A, Haber S, Lozano AM (2011): The subcallosal cingulate gyrus in the context of major depression. Biol Psychiatry 69:301–308.
2. Seminowicz DA, Mayberg HS, McIntosh AR, Goldapple K, Kennedy S, Segal Z, Rafi-Tari S (2004): Limbic-frontal circuitry in major depression: A path modeling metanalysis. Neuroimage 22:409–418.
3. Drevets WC, Savitz J, Trimble M (2008): The subgenual anterior cingulate cortex in mood disorders. CNS Spectr 13:663–681.
4. Morris LS, Costi S, Tan A, Stern ER, Charney DS, Murrough JW (2020): Ketamine normalizes subgenual cingulate cortex hyper-activity in depression. Neuropsychopharmacology 45:975–981.
5. Berlim MT, McGirr A, Van den Eynde F, Fleck MPA, Giacobbe P (2014): Effectiveness and acceptability of deep brain stimulation (DBS) of the subgenual cingulate cortex for treatment-resistant depression: A systematic review and exploratory meta-analysis. J Affect Disord 159:31–38.
6. Figee M, Riva-Posse P, Choi KS, Bederson L, Mayberg HS, Kopell BH (2022): Deep brain stimulation for depression. Neurotherapeutics 19:1229–1245.
7. Johnson KA, Okun MS, Scangos KW, Mayberg HS, de Hemptinne C (2024): Deep brain stimulation for refractory major depressive disorder: A comprehensive review. Mol Psychiatry 29:1075–1087.
8. Mayberg HS, Lozano AM, Voon V, McNeely HE, Seminowicz D, Hamani C, *et al.* (2005): Deep brain stimulation for treatment-resistant depression. Neuron 45:651–660.
9. Fenoy AJ, Simpson RK (2014): Risks of common complications in deep brain stimulation surgery: Management and avoidance. J Neurosurg 120:132–139.
10. Riis T, Feldman D, Mickey B, Kubanek J (2024): Controlled noninvasive modulation of deep brain regions in humans, Communications. Engineering 3:13.
11. Riis T, Feldman D, Losser A, Mickey B, Kubanek J (2024): Device for multifocal delivery of ultrasound into deep brain regions in humans. IEEE Trans Biomed Eng 71:660–668.
12. Riis TS, Feldman DA, Vonesh LC, Brown JR, Solzbacher D, Kubanek J, Mickey BJ (2023): Durable effects of deep brain ultrasonic neuromodulation on major depression: A case report. J Med Case Rep 17:449.
13. Riis TS, Losser AJ, Kassavetis P, Moretti P, Kubanek J (2024): Noninvasive modulation of essential tremor with focused ultrasonic waves. J Neural Eng 21.
14. Darmani G, Bergmann TO, Butts Pauly K, Caskey CF, de Lecea L, Fomenko A, *et al.* (2022): Non-invasive transcranial ultrasound stimulation for neuromodulation. Clin Neurophysiol 135:51–73.

15. Riva-Posse P, Choi KS, Holtzheimer PE, McIntyre CC, Gross RE, Chaturvedi A, *et al.* (2014): Defining critical white matter pathways mediating successful subcallosal cingulate deep brain stimulation for treatment-resistant depression. Biol Psychiatry 76:963–969.
16. Zhang H, Zhang Y, Xu M, Song X, Chen S, Jian X, Ming D (2021): The effects of the structural and acoustic parameters of the skull model on transcranial focused ultrasound. Sensors 21:5962.
17. Sarica C, Nankoo J-F, Fomenko A, Grippe TC, Yamamoto K, Samuel N, *et al.* (2022): Human Studies of transcranial ultrasound neuromodulation: A systematic review of effectiveness and safety. Brain Stimul 15:737–746.
18. Braun V, Blackmore J, Cleveland RO, Butler CR (2020): Transcranial ultrasound stimulation in humans is associated with an auditory confound that can be effectively masked. Brain Stimul 13:1527–1534.
19. Zeng K, Darmani G, Fomenko A, Xia X, Tran S, Nankoo J-F, *et al.* (2022): Induction of human motor cortex plasticity by theta burst transcranial ultrasound stimulation. Ann Neurol 91:238–252.
20. Watson DB, Clark LA (1994): The Panas-X manual for the positive and negative affect schedule. Available at: https://api.semanticscholar.org/CorpusID:17751759. Accessed August 20, 2009.
21. Hamilton M (1960): A rating scale for depression. J Neurol Neurosurg Psychiatry 23:56–62.
22. Bech P, Allerup P, Gram LF, Reisby N, Rosenberg R, Jacobsen O, Nagy A (1981): The Hamilton depression scale. Evaluation of objectivity using logistic models. Acta Psychiatr Scand 63:290–299.
23. O'Sullivan RL, Fava M, Agustin C, Baer L, Rosenbaum JF (1997): Sensitivity of the six-item Hamilton Depression Rating Scale. Acta Psychiatr Scand 95:379–384.
24. Dunlop BW, Parikh SV, Rothschild AJ, Thase ME, DeBattista C, Conway CR, *et al.* (2019): Comparing sensitivity to change using the 6-item versus the 17-item Hamilton depression rating scale in the GUIDED randomized controlled trial. BMC Psychiatry 19:420.
25. Rush AJ, South C, Jain S, Agha R, Zhang M, Shrestha S, *et al.* (2021): Clinically significant changes in the 17- and 6-item hamilton rating scales for depression: A star*D report. Neuropsychiatr Dis Treat 17:2333–2345.
26. Rief W, Barsky AJ, Glombiewski JA, Nestoriuc Y, Glaesmer H, Braehler E (2011): Assessing general side effects in clinical trials: Reference data from the general population. Pharmacoepidemiol Drug Saf 20:405–415.
27. Naor O, Krupa S, Shoham S (2016): Ultrasonic neuromodulation. J Neural Eng 13:031003.
28. Kubanek J (2018): Neuromodulation with transcranial focused ultrasound. Neurosurg Focus 44:E14.
29. Blackmore J, Shrivastava S, Sallet J, Butler CR, Cleveland RO (2019): Ultrasound neuromodulation: A review of results, mechanisms and safety. Ultrasound Med Biol 45:1509–1536.
30. Cobbold RS (2006): Foundations of Biomedical Ultrasound. Oxford, London: Oxford university press.
31. Riis TS, Webb TD, Kubanek J (2022): Acoustic properties across the human skull. Ultrasonics 119:106591.
32. Riva-Posse P, Choi KS, Holtzheimer PE, Crowell AL, Garlow SJ, Rajendra JK, *et al.* (2018): A connectomic approach for subcallosal cingulate deep brain stimulation surgery: Prospective targeting in treatment-resistant depression. Mol Psychiatry 23:843–849.
33. Hameroff S, Trakas M, Duffield C, Annabi E, Gerace MB, Boyle P, *et al.* (2013): Transcranial ultrasound (tus) effects on mental states: A pilot study. Brain Stimul 6:409–415.
34. Sanguinetti JL, Hameroff S, Smith EE, Sato T, Daft CMW, Tyler WJ, Allen JJB (2020): Transcranial focused ultrasound to the right prefrontal cortex improves mood and alters functional connectivity in humans. Front Hum Neurosci 14:52.
35. Reznik SJ, Sanguinetti JL, Tyler WJ, Daft C, Allen JJB (2020): A double-blind pilot study of transcranial ultrasound (TUS) as a five-day intervention: TUS mitigates worry among depressed participants. Neurol Psychiatry Brain Res 37:60–66.
36. Kaye EA, Pauly KB (2013): Adapting MRI acoustic radiation force imaging for in vivo human brain focused ultrasound applications. Magn Reson Med 69:724–733.
37. Manduca A, Bayly PJ, Ehman RL, Kolipaka A, Royston TJ, Sack I, *et al.* (2021): MR elastography: Principles, guidelines, and terminology. Magn Reson Med 85:2377–2390.